Research Square

Preprints are preliminary reports that have not undergone peer review.
They should not be considered conclusive, used to inform clinical practice,
or referenced by the media as validated information.

An Application of State-Space Approach forSoil-Structure Interaction Under Seismic Excitation

Patricia Grezelle
Federal University of Technology – Paraná
Ana Raquel Pessa
anapessa@alunos.utfpr.edu.br
Federal University of Technology – Paraná
Matheus Wessling
Federal University of Technology – Paraná
Francisco Augusto Aparecido Gomes
Federal University of Technology – Paraná
Paôla Regina Dalcanal
Federal University of Technology – Paraná
Paulo Rogerio Novak
Federal University of Technology – Paraná

Research Article

Keywords: State-Space method, Soil-structure interaction, Seismic excitation, Dynamic analysis, Frequency-domain response

Posted Date: May 28th, 2026

DOI: https://doi.org/10.21203/rs.3.rs-9696218/v1

License: This work is licensed under a Creative Commons Attribution 4.0 International License.
Read Full License

Additional Declarations: No competing interests reported.

An Application of State-Space Approach for Soil-Structure Interaction Under Seismic Excitation

Patricia Grezelle[1], Ana Raquel Pessa[1*], Matheus Wessling[1], Francisco Augusto Aparecido Gomes[1,3], Paôla Regina Dalcanal[2], Paulo Rogerio Novak[1,3]

[1]Civil Engineering Graduate Program (PPGEC-PB), Department of Civil Engineering, Universidade Tecnológica Federal do Paraná, Pato Branco, PR, Brazil.
[2]Department of Civil Engineering, Universidade Tecnológica Federal do Paraná, Pato Branco, PR, Brazil.
[3]Department of Mechanical Engineering, Universidade Tecnológica Federal do Paraná, Pato Branco, PR, Brazil.

*Corresponding author(s). E-mail(s): anapessa@alunos.utfpr.edu.br;

Abstract

Soil-structure interaction (SSI) plays a fundamental role in the dynamic response of coupled soil-foundation-structure systems subjected to seismic loading. Depending on the mechanical properties of the soil and the structural characteristics, SSI effects may either amplify or attenuate structural vibrations. Although these problems are commonly solved using direct numerical approaches, many practical cases can be efficiently represented by systems of ordinary differential equations. In this study, an application of state-space approach is proposed for the dynamic analysis of two-dimensional SSI systems under seismic excitation, aiming to reduce computational cost while maintaining numerical accuracy. The formulation was initially validated using one- and two-degree-of-freedom models through comparisons with analytical solutions and fourth-order Runge-Kutta methods. Subsequently, the proposed framework was applied to three structural models with different heights, representing buildings with 3, 7, and 15 stories, subjected to historical earthquake records. Time-domain responses in terms of displacement, velocity, and acceleration were obtained, and Fast Fourier Transform analyses were performed to evaluate the frequency-domain behaviour. The results demonstrated excellent agreement with reference solutions, high numerical stability, and substantially lower computational time when compared with

conventional iterative procedures, indicating that the proposed method is an efficient and reliable alternative for SSI dynamic analysis.

Keywords: State-Space method, Soil-structure interaction, Seismic excitation, Dynamic analysis, Frequency-domain response

1 Introduction

Seismic events, explosions, intense traffic, and rotating machinery are typical sources of vibrations transmitted to structures directly or indirectly. The intensity of these vibrations dictates the extent of the damage they can cause, ranging from negligible to catastrophic structural failure. Structures are increasingly exposed to dynamic forces, whether anthropogenic or natural [1]. Among these, seismic actions are particularly significant. As noted by Wolf [2], earthquakes result from energy release along geological faults. Consequently, analyzing Soil-Structure Interaction (SSI) is essential, as the soil modifies the structural response while the movement of the structure simultaneously influences the soil behaviour.

The advent of advanced computational technologies has led to a notable upsurge in research activity concerning SSI problems. Contemporary methodologies permit the analysis of flexible, irregularly shaped foundations embedded in inhomogeneous or layered media, as well as soil inelasticity [3]. Furthermore, recent literature underscores the growing concern regarding the dynamic behaviour of structures under seismic excitations [4–6].

Commonly, SSI problems are addressed through direct methods. Wolf [7] describes a simplified approach that utilizes lumped mass-spring-damper systems. In such cases, the governing equations of motion, derived from Newton's second law, can be efficiently solved using the State-Space method.

The State-Space method, widely adopted in control engineering since the pioneering work of Kalman in 1960 [8], consists of state and output equations solved through matrix operations in the time domain [9]. This approach determines all achievable states and their transitions, representing them in a directed graphical manner [10]. Historically, the method was instrumental in aerospace programs such as Apollo and Polaris [8, 11, 12].

Analyzing SSI can demand high computational costs, particularly in direct methods where the soil-structure interface involves a large number of degrees of freedom (DOF) [2, 3, 13, 14]. In this context, this article investigates the State-Space method for coupled SSI and seismic excitation problems as a computationally efficient alternative for fundamental analyses. A primary advantage of this method is the flexibility in choosing state variables; for complex multi-input multi-output (MIMO) systems, the State-Space approach is especially advantageous [9], as system behaviour can be modeled algorithmically to facilitate error identification [10].

The present study uses the State-Space approach, coupled with SSI problems, to evaluate two- and three-dimensional structures with 3, 7, and 15 stories, considering flexural vibration. To validate the algorithm, the code was initially tested against two

dynamic problems with 1 (Case 1) and 2 (Case 2) DOFs. The results of Case 1 were compared with analytical solutions, while Case 2 was validated using the Runge-Kutta method. All models were implemented in *MATLAB*® [15], with results presented in the time domain for all scenarios and in the frequency domain for SSI cases.

The generalization of the State-Space method aims to contribute to studies involving soil–structure interaction (SSI) and seismic excitation by proposing an efficient and accurate computational alternative for structural analysis. Considering that damage caused by earthquakes can be catastrophic, such as the 1994 Northridge earthquake in Los Angeles (USA), which is considered one of the most expensive natural disasters in history, economic losses were estimated at approximately 40 billion [16]. Due to the significant impact of this event, several studies have been conducted to analyze structural behaviour and develop strategies to mitigate seismic effects [17, 18].

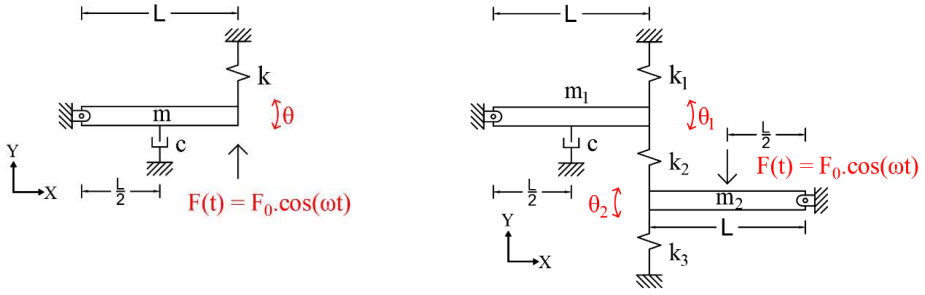
2 Problem Description and Formulation

2.1 Discrete models of systems with 1 DOF and 2 DOF

Figure 1 presents the two dynamic problems addressed in this study: a system with one degree of freedom (1 DOF), referred to as Case 1, and a system with two degrees of freedom (2 DOF), referred to as Case 2.

For Case 1 (Figure 1(a)), the discrete model consists of a concentrated mass connected to a pivot, a viscous damper (c), and a spring with stiffness (k). The system is subjected to a harmonic force $F(t)$, and θ represents the angular displacement.

In Case 2 (Figure 1(b)), the system is composed of two masses (m_1 and m_2) connected by pivots, one viscous damper (c), and three stiffness elements (k_1, k_2, and k_3), also subjected to a harmonic excitation force $F(t)$.



(a) (b)

Fig. 1 Discrete benchmark models used for validation: (a) one-degree-of-freedom system (Case 1); (b) two-degree-of-freedom system (Case 2).

The equations of motion that describe the models presented in Figure 1 are derived from Newton's second law. The formulation for Case 1 (Figure 1(a)) is given by Eq. (1), while the formulation for Case 2 (Figure 1(b)) is given by Eq. (2).

$$I_0\ddot{\theta} + \frac{cL^2}{4}\dot{\theta} + kL^2\theta = F_0 L\cos(\omega t) \tag{1}$$

where I_0, c, and k are the mass moment of inertia (kg·m^2), damping coefficient (Ns/m) and stiffness (N/m), respectively $\ddot{\theta}$, $\dot{\theta}$, and θ represent angular acceleration (rad/s^2), angular velocity (rad / s) and angular displacement (rad), respectively. L is the length of the lever arm, F_0 is the force amplitude (N), ω is the excitation frequency (rad/s), and t is the time (s).

$$\begin{bmatrix} I_{01} & 0 \\ 0 & I_{02} \end{bmatrix} \begin{Bmatrix} \ddot{\theta}_1 \\ \ddot{\theta}_2 \end{Bmatrix} + \begin{bmatrix} \frac{cL^2}{4} & 0 \\ 0 & 0 \end{bmatrix} \begin{Bmatrix} \dot{\theta}_1 \\ \dot{\theta}_2 \end{Bmatrix} + \begin{bmatrix} (k_1+k_2)L^2 & -k_2L^2 \\ -k_2L^2 & (k_2+k_3)L^2 \end{bmatrix} \begin{Bmatrix} \theta_1 \\ \theta_2 \end{Bmatrix} = \begin{Bmatrix} 0 \\ \frac{F_0 L}{2}\cos(\omega t) \end{Bmatrix} \tag{2}$$

Subscripts 1 and 2 refer to bodies 1 and 2 shown in Figure 1(b), respectively. The parameter I denotes the mass moment of inertia, c the damping coefficient, and k the stiffness. The variables $\ddot{\theta}$, $\dot{\theta}$, and θ represent angular acceleration, velocity, and displacement, respectively. L is the lever arm length, ω is the excitation frequency, and t is time.

2.2 Discrete model of structures with 3, 7 and 15 floors

To demonstrate the generalization of the state-space formulation, three discrete models with concentrated masses are analysed, as shown in Figure 2. The structures are assumed to be metallic, two-dimensional, and constrained to vibrate in the plane under flexural behaviour.

The excitation force is applied along the X-axis, considering the XY Cartesian coordinate system. Figure 2(a) represents the 3-story structure, Figure 2(b) the 7-story structure, and Figure 2(c) the 15-story structure. All models include soil–structure interaction, with the structures coupled to the ground. The soil is modeled as a homogeneous, isotropic, linear elastic half-space. The variable H denotes the height of each floor relative to the ground surface. The subscripts f and N refer to the foundation and the structural floors, respectively.

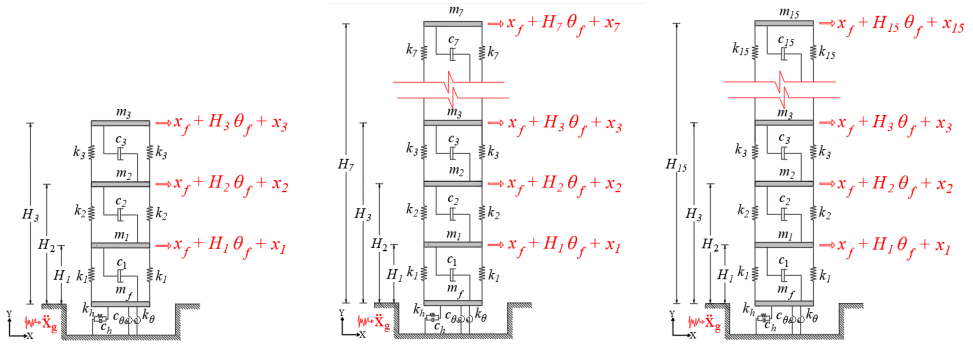


Fig. 2 Multi-story structural models with soil–structure interaction: (a) 3-story structure; (b) 7-story structure; (c) 15-story structure.

The equation of motion for the coupled soil-structure system, derived from Newton's second law, is presented in Eq. (3).

$$\mathbf{M}_{se}\,\ddot{\mathbf{x}}_{se}(t) + \mathbf{C}_{se}\,\dot{\mathbf{x}}_{se}(t) + \mathbf{K}_{se}\,\mathbf{x}_{se}(t) = -\mathbf{G}\,\ddot{\mathbf{x}}_{g}(t) \tag{3}$$

where $\mathbf{M}_{se}$, $\mathbf{C}_{se}$, and $\mathbf{K}_{se}$ are the soil-structure mass, damping, and stiffness matrices, respectively. The vectors $\ddot{\mathbf{x}}_{se}(t)$, $\dot{\mathbf{x}}_{se}(t)$, and $\mathbf{x}_{se}(t)$ represent the soil-structure acceleration, velocity, and displacement responses, respectively. The variable t denotes time. The matrix $\mathbf{G}$ represents the ground impedance, and $\ddot{\mathbf{x}}_{g}(t)$ is the ground acceleration vector associated with the seismic excitation.

2.3 Mathematical Formulation

Two different solution approaches were adopted to validate the proposed model. For Case 1, an analytical solution is employed, while for Case 2, a numerical solution based on the fourth-order Runge–Kutta method is used.

The analytical solution of Eq. (1) leads to the expressions for angular displacement and angular velocity, given by Eqs. (4) and (5), respectively.

$$\theta(t) = A_h e^{-\xi\omega_n t}\cos(\omega_d t - \phi) + A_0\cos(\omega t - \phi_0) \tag{4}$$

$$\dot{\theta}(t) = -\xi\omega_n A_h e^{-\xi\omega_n t}\cos(\omega_d t - \phi) - \omega_d A_h e^{-\xi\omega_n t}\sin(\omega_d t - \phi) + A_0\omega\sin(\omega t - \phi_0) \tag{5}$$

where A_h is the amplitude of the homogeneous solution, ξ is the damping ratio, ω_n is the natural frequency, and ω_d is the damped natural frequency. The parameter ϕ is the phase angle, while A_0 and ϕ_0 are constants determined from the initial conditions.

Equation (2) is solved numerically using the fourth-order Runge–Kutta (RK4) method. For this purpose, the system is first rewritten as a set of first-order differential equations. The corresponding state-space representation is given in Eq. (6).

$$\begin{aligned}
\dot{x}_1 &= x_2 \\
\dot{x}_2 &= \frac{-\frac{cL^2}{4}x_2 - (k_1+k_2)L^2x_1 + k_2L^2x_3}{I_{01}} \\
\dot{x}_3 &= x_4 \\
\dot{x}_4 &= \frac{F(t) + k_2L^2x_1 - (k_2+k_3)L^2x_3}{I_{02}}
\end{aligned} \tag{6}$$

The RK4 method advances the solution through four intermediate evaluations at each time step. The general update expression is given by Eq. (7).

$$y_{i+1} = y_i + \frac{h}{6}\left(k_1 + 2k_2 + 2k_3 + k_4\right) \tag{7}$$

The intermediate slopes are defined in Eq. (8).

$$
\begin{aligned}
k_1 &= f(x_i, y_i) \\
k_2 &= f\left(x_i + \frac{h}{2},\, y_i + \frac{h}{2}k_1\right) \\
k_3 &= f\left(x_i + \frac{h}{2},\, y_i + \frac{h}{2}k_2\right) \\
k_4 &= f(x_i + h,\, y_i + hk_3)
\end{aligned}
\tag{8}
$$

where k_1, k_2, k_3, and k_4 represent the intermediate slopes, and h is the integration time step. Equation (7) corresponds to a weighted average of these slopes, providing improved accuracy in the numerical solution.

Modeling in the state-space framework consists of two sets of equations: the state equation and the output equation. For a linear time-invariant (LTI) system, the mathematical representation is given by Eqs. (9) and (10).

$$\dot{\mathbf{z}}(t) = \mathbf{A}\mathbf{z}(t) + \mathbf{B}\mathbf{u}(t) \tag{9}$$

$$\mathbf{y}(t) = \mathbf{C}\mathbf{z}(t) + \mathbf{D}\mathbf{u}(t) \tag{10}$$

where $\mathbf{z}(t) \in \mathbb{R}^n$ is the state vector, $\dot{\mathbf{z}}(t)$ is its time derivative, $\mathbf{y}(t) \in \mathbb{R}^m$ is the output vector, and $\mathbf{u}(t) \in \mathbb{R}^r$ is the input vector. The matrix $\mathbf{A} \in \mathbb{R}^{n\times n}$ is the state (or system) matrix, $\mathbf{B} \in \mathbb{R}^{n\times r}$ is the input matrix, $\mathbf{C} \in \mathbb{R}^{m\times n}$ is the output matrix, and $\mathbf{D} \in \mathbb{R}^{m\times r}$ is the direct transmission matrix [9, 19–21].

The solution of Eq. (9) provides the time response of all state variables. Once the state vector $\mathbf{z}(t)$ is known, the output vector $\mathbf{y}(t)$ can be directly obtained from Eq. (10). Therefore, both time-domain and frequency-domain analyses enable a complete characterization of the system behaviour [22].

The state-space formulation for soil–structure interaction (SSI) problems based on the mass–spring–damper model is presented in Eqs. (11)–(12).

$$\dot{\mathbf{z}}(t) = \mathbf{A}\mathbf{z}(t) + \mathbf{B}\ddot{\mathbf{x}}_g(t) \tag{11}$$

$$\mathbf{y}(t) = \mathbf{C}\mathbf{z}(t) \tag{12}$$

The state vector is defined in Eq. (13).

$$\mathbf{z}(t) = \left\{\mathbf{x}_{se}(t)\ \ \dot{\mathbf{x}}_{se}(t)\right\} \tag{13}$$

The system matrices are given by Eqs. (14)–(16).

$$\mathbf{A} = \begin{bmatrix} \mathbf{0} & \mathbf{I} \\ -\mathbf{M}_{se}^{-1}\mathbf{K}_{se} & -\mathbf{M}_{se}^{-1}\mathbf{C}_{se} \end{bmatrix} \tag{14}$$

$$\mathbf{B} = \begin{bmatrix} \mathbf{0} \\ -\mathbf{M}_{se}^{-1}\mathbf{v}_{se} \end{bmatrix} \tag{15}$$

$$\mathbf{C} = \begin{bmatrix} \mathbf{I} & \mathbf{0} \\ \mathbf{0} & \mathbf{I} \\ -\mathbf{M}_{se}^{-1}\mathbf{K}_{se} & -\mathbf{M}_{se}^{-1}\mathbf{C}_{se} \end{bmatrix} \tag{16}$$

The output vector is defined in Eq. (17).

$$\mathbf{y}(t) = \left\{\mathbf{x}_{se}(t)\ \dot{\mathbf{x}}_{se}(t)\ \ddot{\mathbf{x}}_{se}(t)\right\} \tag{17}$$

2.4 Solution Scheme

The generalized implementation of the state-space model follows a structured sequence of steps. Initially, the input parameters of the structure are defined, including mass, geometric properties, Young's modulus, Poisson's ratio, material density, interstory height, moment of inertia, number of floors, time step, and damping ratio.

Subsequently, the structural mass and stiffness matrices are assembled. The damping matrix is obtained using either the Rayleigh or Caughey formulations, depending on the adopted approach.

The soil matrices are then determined from the soil properties, such as the Poisson ratio, shear modulus, foundation radius, soil density, wave propagation velocity, and foundation mass, as well as the relative position of each floor with respect to the base. Based on structural and soil data, coupled soil-structure matrices are constructed, including the interaction mass matrix $\mathbf{M}_{se}$.

Once the coupled system matrices are established, the state-space matrices are formulated. The dynamic response is then computed, and the results are stored in the output vector $\mathbf{y}(t)$. After obtaining the time-domain response, the Fast Fourier Transform (FFT) is applied to determine the corresponding frequency-domain response.

The overall solution procedure is illustrated in Figure 3.

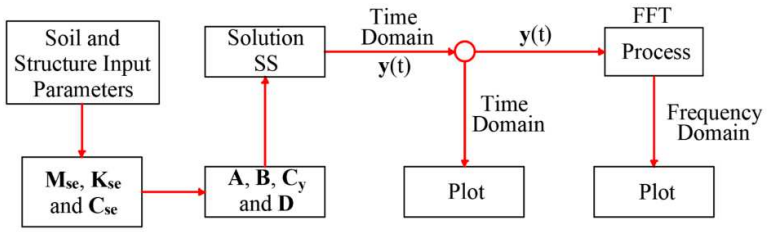


Fig. 3 Flowchart of the generalized state-space solution procedure for SSI dynamic analysis.

The simulations were performed using *MATLAB*® [15] on a notebook equipped with an Intel Core i7-7700HQ processor (2.80 GHz, 4 cores, 8 threads), 32 GB of DDR4 RAM, and an NVIDIA GTX 1060 graphics card with 6 GB of memory.

3 Results

To demonstrate the generalization of the state-space approach for two-dimensional problems undergoing flexural vibration, two initial models are considered: Case 1 and Case 2. These models are used to evaluate the accuracy of the method in solving dynamic problems.

Subsequently, the proposed formulation is applied to two-dimensional structures involving soil–structure interaction (SSI) under seismic excitation, considering buildings with 3, 7, and 15 stories.

3.1 Harmonically damped system

Case 1 was solved both analytically and using the state-space approach. The system properties adopted in the simulations are summarized in Table 1.

Table 1 System properties with 1 DOF - Case 1.

Case 1 - Properties	**Numerical Values**
θ_0	0
$\dot{\theta}_0$	0
m	2.54 kg
k	27040 N/m
L	0.7 m
I_0	$\frac{mL^3}{3} = 0.4149 \text{ kg} \cdot \text{m}^2$
t	$0 : 0.001 : 4$ s
ξ	0.0061
ω_n	$L\sqrt{\frac{k}{I_0}} = 178.71$ rad/s (28.44 Hz)
ω	ω_n
$F(t)$	$F_0 \cos(\omega t)$
F_0	1 N
c	$2\xi\omega_n I_0 = 0.9045 \text{ N} \cdot \text{s/m}$

The mass, stiffness, and damping properties were obtained from an experimental system available at the Vibrations Laboratory of the Federal University of Technology - Paraná (UTFPR-PB), located in Pato Branco. The damping factor for Case 1 was determined experimentally.

The responses in the time-domain are presented in Figures 4 and 5, corresponding to the angular displacement and the angular velocity, respectively.

A comparison between the analytical and State-Space solutions shows a strong agreement between the responses. This behaviour is observed for both angular displacement (Figure 4) and angular velocity (Figure 5). Therefore, the State-Space approach proved to be accurate and suitable for solving this problem.

Case 2 was analysed by comparing the Runge–Kutta methods implemented through the `ode23` and `ode45` functions of *MATLAB*® [15]. Both numerical solutions were correlated with the response obtained using the State-Space approach. The properties adopted for Case 2 are summarized in Table 2.

The natural frequencies of the system are obtained from the characteristic equation given by Eq. (18).

$$\frac{38725729}{75000000}\omega^4 - \frac{360728641}{12500}\omega^2 + \frac{3840197816}{25} = 0 \tag{18}$$

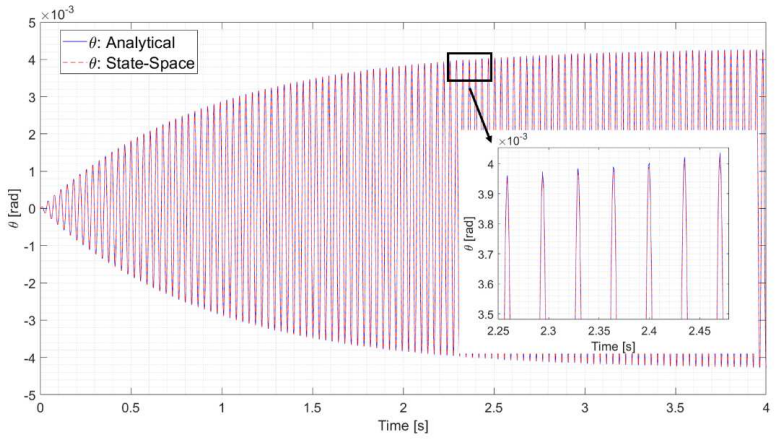


Fig. 4 Time-domain angular displacement response for Case 1 under harmonic excitation.

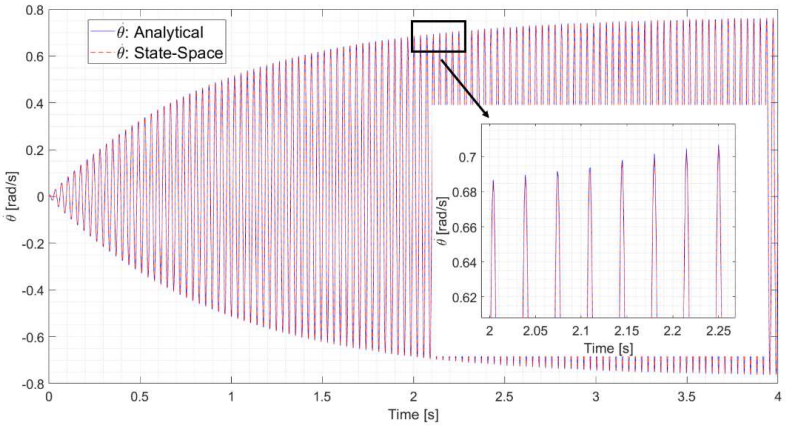


Fig. 5 Time-domain angular velocity response for Case 1 under harmonic excitation.

The natural frequency responses for Case 2 are presented in Table 3.

Figures 6 and 8 show the angular displacement of bodies 1 and 2, respectively, while Figs. 7 and 9 present the corresponding angular velocities.

Table 2 System properties with 2 DOF - Case 2.

Case 2 - Properties	**Numerical values**
$\theta_{01} = \theta_{02}$	0
$\dot{\theta}_{01} = \dot{\theta}_{02}$	0
m_1	2.54 kg
m_2	7.62 kg
k_1	27040 N/m
k_2	13520 N/m
k_3	6760 N/m
L	0.7 m
I_1	$\frac{m_1 L^3}{3} = 0.4149$ kg $\cdot$ m^2
I_2	$\frac{m_2 L^3}{3} = 1.2446$ kg $\cdot$ m^2
t	$0 : 0.001 : 4$ s
ξ	0.0061
ω_n	$L\sqrt{\frac{k}{I_0}} = 178.71$ rad/s $(28.44$ Hz$)$
ω	ω_n
$F(t)$	$F_0 \cos(\omega t)$
F_0	1 N
c	$\xi \left(\frac{2\omega_{n1} I_1}{(L/2)^2} \right) = 3.1369$ N $\cdot$ s/m

Table 3 Natural frequency response for Case 2.

Frequency	**Value (Hz)**
f_{n1}	12.28
f_{n2}	35.56

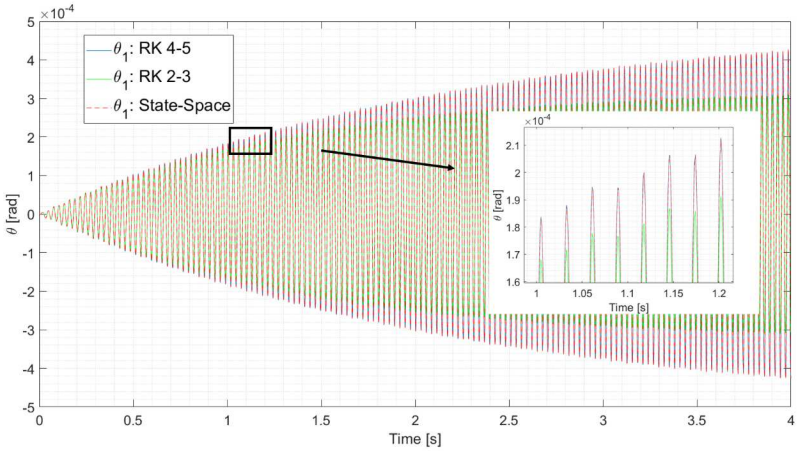


Fig. 6 Time-domain angular displacement response of body 1 for Case 2 under harmonic excitation.

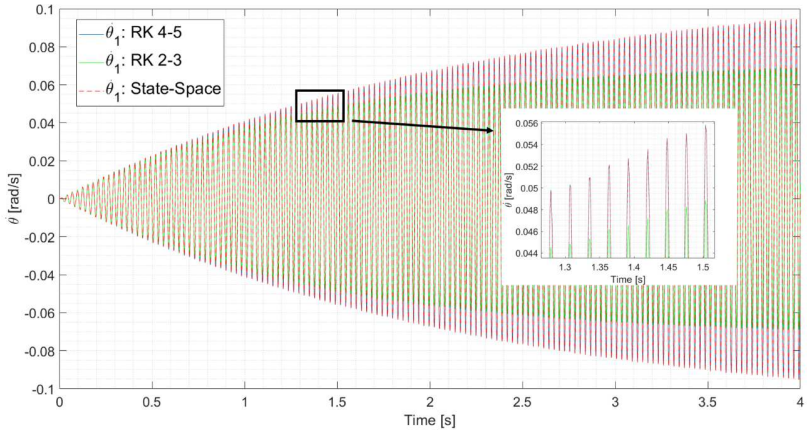


Fig. 7 Time-domain angular velocity response of body 1 for Case 2 under harmonic excitation.

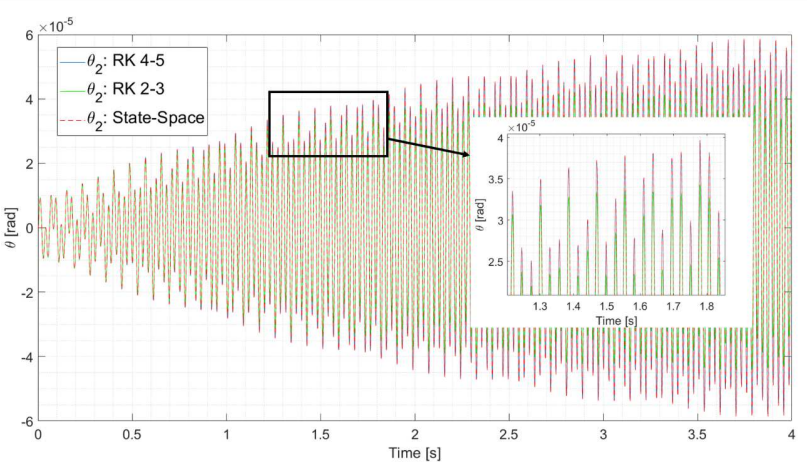


Fig. 8 Time-domain angular displacement response of body 2 for Case 2 under harmonic excitation.

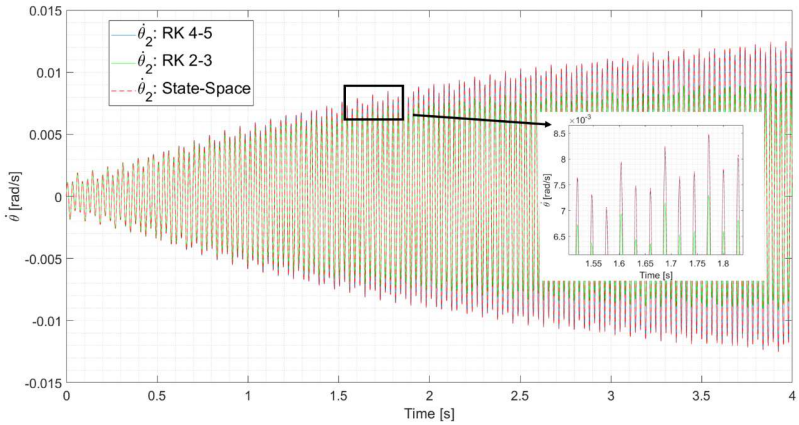


Fig. 9 Time-domain angular velocity response of body 2 for Case 2 under harmonic excitation.

According to Gilat and Subramaniam [23] and Chapra and Canale [24], truncation errors in Runge-Kutta (RK) methods typically decrease as the order of the method increases; thus, higher-order schemes yield superior numerical accuracy. Consequently, as illustrated in Figures 6 through 9, the state-space solution closely aligns with the higher-order RK results, representing the most accurate response among the evaluated methods.

3.2 Seismic excitation in models coupled with SSI

The generalization of the state-space formulation for Soil-Structure Interaction (SSI) and seismic excitation was initially evaluated by analyzing the method's performance under harmonic excitation. This preliminary stage aimed to correlate the results with established numerical methods in the literature, specifically the Runge-Kutta (RK) scheme.

To demonstrate the robustness of the proposed framework, three two-dimensional structures with varying heights (3, 7, and 15 stories) were modeled. The physical properties of the soil and structural components are summarized in Table 4. Following Bowles [25], the soil is characterized as a homogeneous, isotropic, linear elastic half-space.

Table 4 Soil and structure properties.

System properties	**Numerical values**
$\rho_{\text{structural steel}}$	7850 kg/m^3
Soil specific weight	16000 N/m^3
Shear modulus G_{soil}	5.4×10^6 N/m^2
Wave velocity V_s	57.3 m/s
Poisson's ratio v_s	0.4
Young's modulus $E_{\text{structure}}$	2×10^{11} Pa
Distance between floors h	0.3 m
Damping factor ξ	0.01
t	$0 : 0.005 : 47.79$ s
Initial condition z_0	0

In the 7-story model, it was assumed that the floors had uniform mass and stiffness. However, for the 15-story structure, the first three stories were assigned masses three times that of a typical floor (stories 4 through 14), while the top floor was assigned a mass factor of 1.26. This mass distribution in the theoretical models follows an analogy with conventional buildings, where the lower levels serve as parking garages and the roof accommodates additional loads, such as a swimming pool. Floors with identical mass properties are categorized as a typical story type. The coefficients used for mass calculations were based on the ABNT NBR 6120 [26] standard.

The surface foundation adopted for this study is a mat foundation. The analytical model accounts for the mass, inertia, stiffness, and the soil's effective radius. The selection of the type and structural dimensions of the foundation was informed by experimental setups at the UTFPR-PR Mechanical Engineering Vibration Laboratory.

Regarding seismic excitation, the 1994 Northridge earthquake (Los Angeles, USA) was selected as the input signal. The record was retrieved from the PEER Ground Motion Database [27]. Figure 10 presents the ground acceleration time history, recorded at the LA - Sepulveda VA Hospital station (component NORTHR SPV360.AT2). The record features a sampling interval of 0.005 s, a moment magnitude (M_w) of 6.7, a Peak Ground Acceleration (PGA) of -0.932g, and a Joyner-Boore distance of 8.44 km from the epicenter.

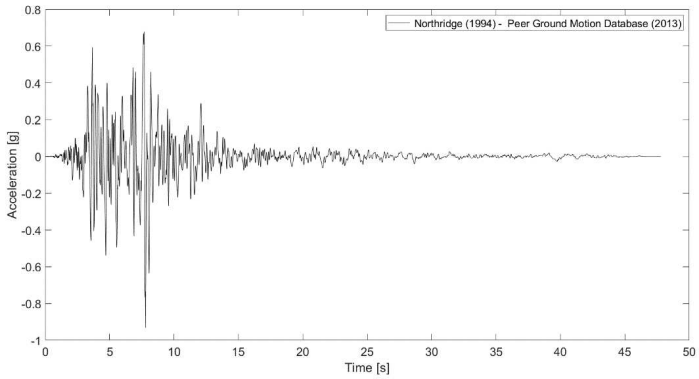


Fig. 10 Ground acceleration record of the 1994 Northridge earthquake used as seismic input excitation. Source: PEER Ground Motion Database [27]

The geometric properties and dimensions for each structural configuration are detailed in Table 5, while the geotechnical parameters of the soil are summarized in Table 6. For the analytical model, the mat foundation is represented by an equivalent circular footing; the corresponding radius (r) is derived from the total contact area of the foundation to ensure consistency in the impedance functions of the soil-structure interaction (SSI).

The matrices $\mathbf{A}$, $\mathbf{B}$, $\mathbf{C}_y$, and $\mathbf{D}$ are assembled by the solution algorithm based on the properties of the material and geometric characteristics of each system. The matrix $\mathbf{D}$ is null, as no direct input is applied to the output.

The modal responses, considering the first three vibration modes of the structures with 3, 7, and 15 stories, are presented in Figure 11. An evident reduction in natural frequencies is observed as the number of stories increases, which is associated with the increase in global flexibility of the structural system. Furthermore, the mode shapes show progressively smoother and more distributed deformation profiles along the height, indicating a growing dominance of the fundamental mode in the dynamic behavior of taller structures.

Figures 12 to 20 illustrate the time-domain responses, including relative displacement, velocity, and acceleration. These results were obtained using the generalized State-Space formulation, considering seismic excitation applied at the base and the influence of soil–structure interaction (SSI).

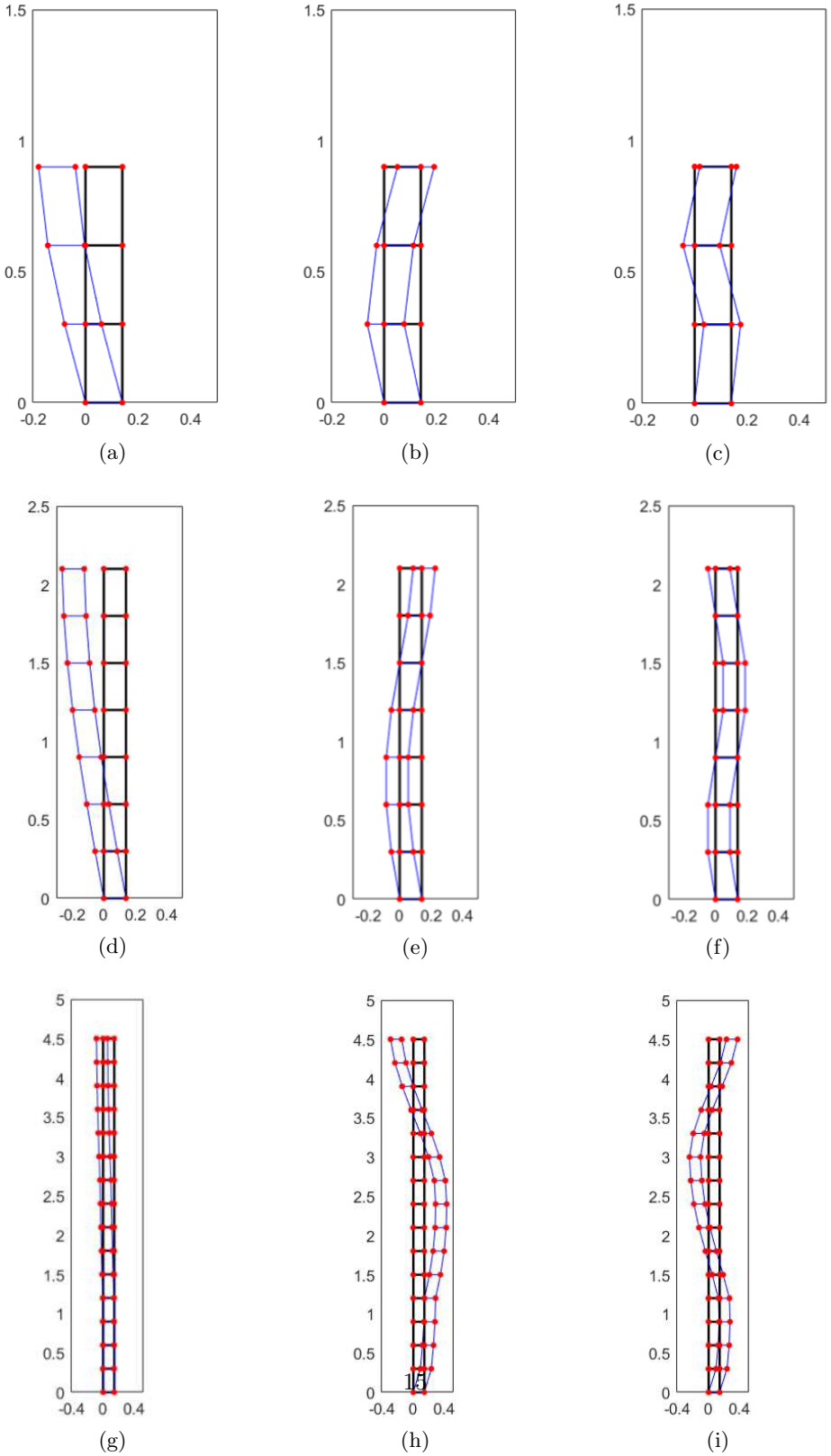


Fig. 11 Modal shapes of the SSI-coupled structures. Top row: 3-story structure (first three modes: 6.58 Hz, 18.43 Hz, 26.64 Hz). Middle row: 7-story structure (3.09 Hz, 9.14 Hz, 14.78 Hz). Bottom row: 15-story structure (0.83 Hz, 2.05 Hz, 2.72 Hz). Mode shapes are scaled for visualization purposes.

Table 5 Structure dimensions, mass and rigidity.

Structure	**3-story structure**	**7-story structure**	**15-story structure**
Total height	0.9 m	2.1 m	4.5 m
Partial height		0.3 m	
Slab Dimensions		0.14 m × 0.012 m × $8{\times}10^{-4}$ m (C×L×E)[1]	
Foundation dimensions		0.1416 m × 0.012 m × $8{\times}10^{-4}$ m (C×L×E)[1]	
Radius		0.0233 m	
Foundations mass		[2]0.0107 kg	
Mass (m)	[2]0.0106 kg	[2]0.0106 kg	[3]0.0106 kg
Stiffness (k)	[2]91.022 N/m	[2]91.022 N/m	[4]91.022 N/m

[1] C is length, L is width and E is thickness.
[2] Same for all floors.
[3] The first 3 floors are $m \times 3$, the last is $m \times 1.26$ and the central ones are equal to m.
[4] The first 5 floors are $k \times 3$, the last 5 are $k/2$ and the central ones are equal to k.

Table 6 Soil stiffness and damping.

	Translational (k_h, c_h)	**Rotational** (k_θ, c_θ)
Stiffness (N/m)	627929.776	301.8930964
Damping (Ns/m)	1425.630836	0.178802093

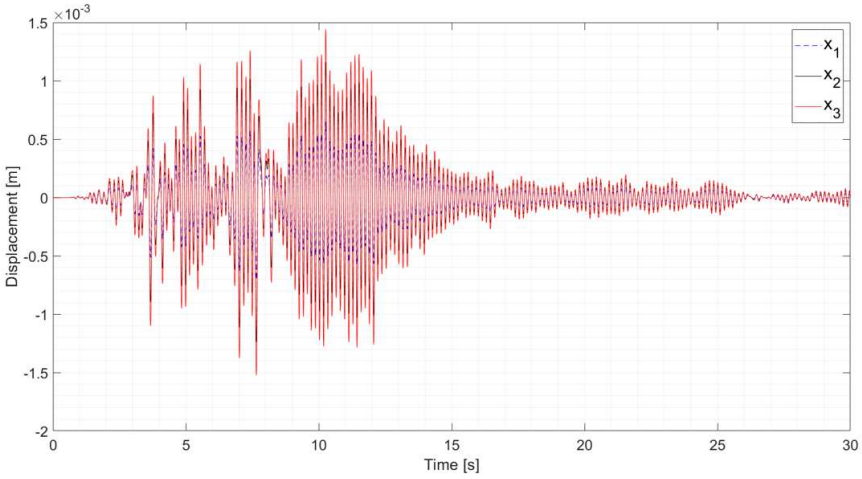


Fig. 12 Time-domain response of displacement along the height of the 3-story structure under seismic excitation considering soil-structure interaction (SSI).

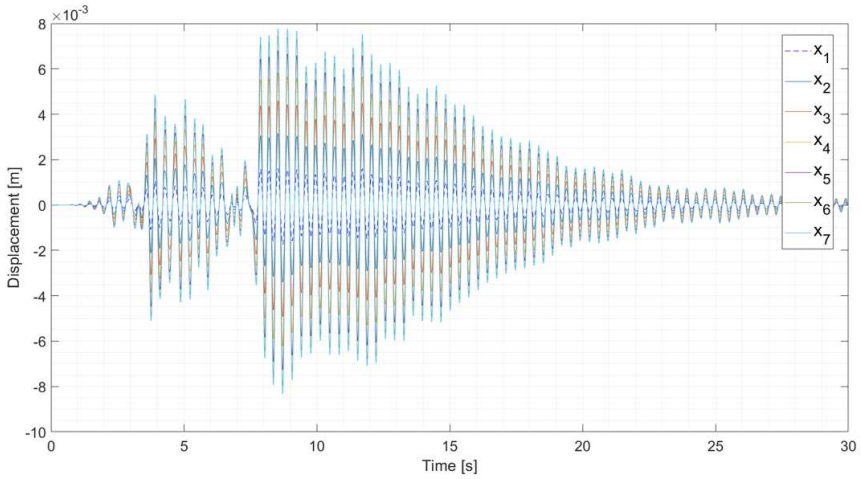


Fig. 13 Time-domain response of displacement along the height of the 7-story structure under seismic excitation considering soil-structure interaction (SSI).

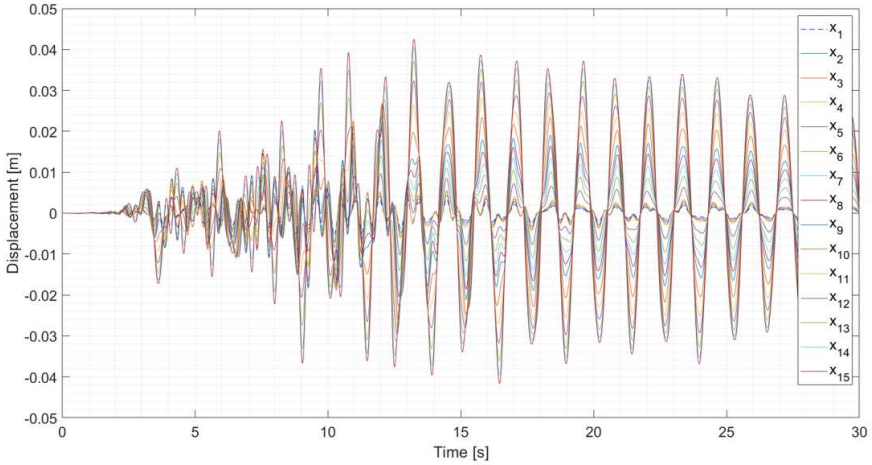


Fig. 14 Time-domain response of displacement along the height of the 15-story structure under seismic excitation considering soil-structure interaction (SSI).

When analyzing Figures 12 to 20, it can be observed that the maximum amplitudes occur at the top floor for all structures. Table 7 summarizes the peak responses.

Table 7 Responses of maximum amplitudes of displacement, velocity and acceleration in the time-domain.

	3-story structure	**7-story structure**	**15-story structure**
Displacement	-0.001523 m	-0.008333 m	0.04247 m
Velocity	0.05346 m/s	0.1462 m/s	-0.3395 m/s
Acceleration	-2.09 m/s^2	2.914 m/s^2	-3.742 m/s^2

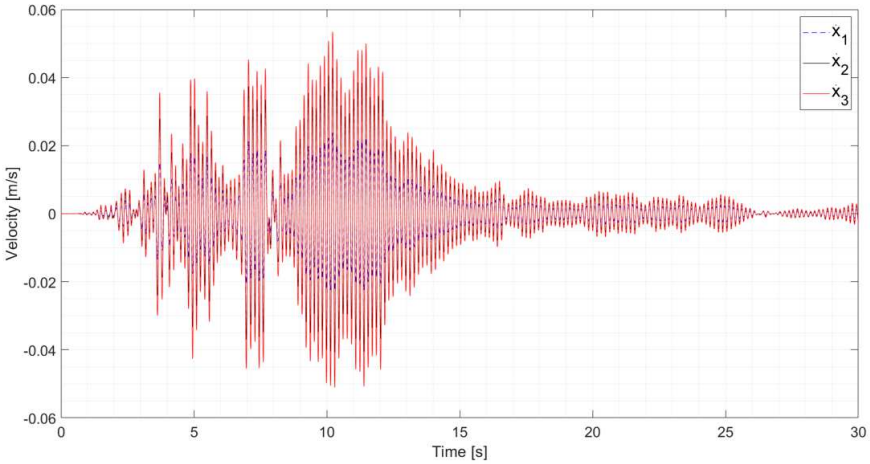


Fig. 15 Time-domain response of velocity along the height of the 3-story structure under seismic excitation considering soil-structure interaction (SSI).

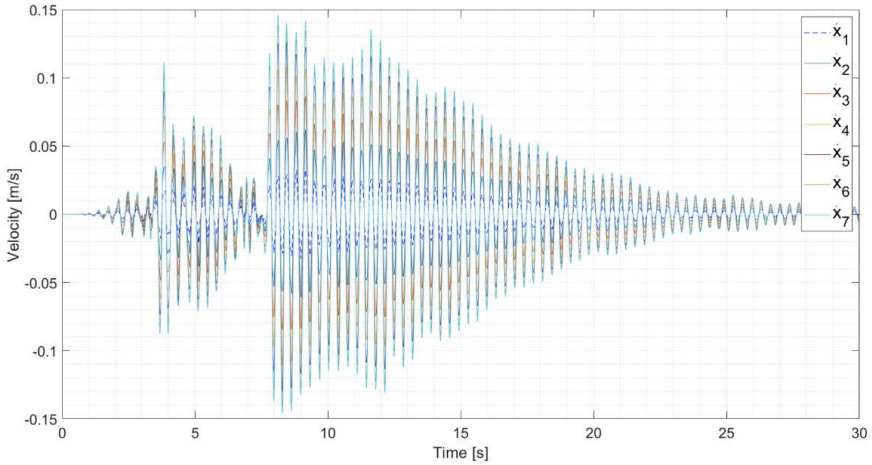


Fig. 16 Time-domain response of velocity along the height of the 7-story structure under seismic excitation considering soil-structure interaction (SSI).

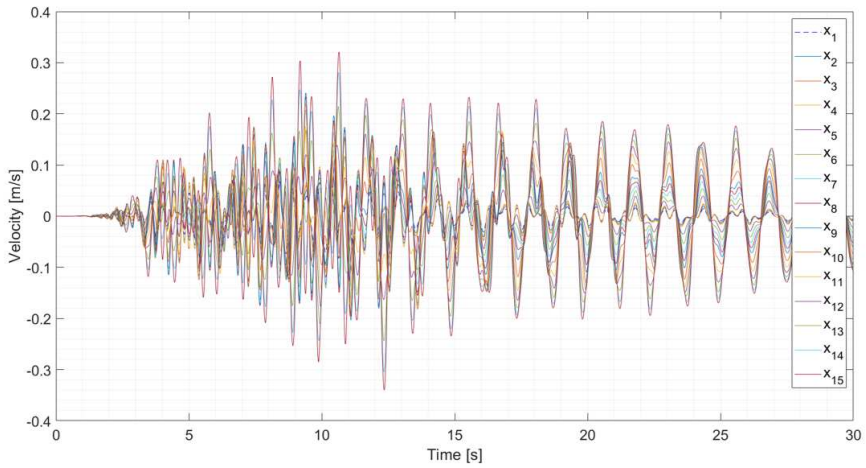


Fig. 17 Time-domain response of velocity along the height of the 15-story structure under seismic excitation considering soil-structure interaction (SSI).

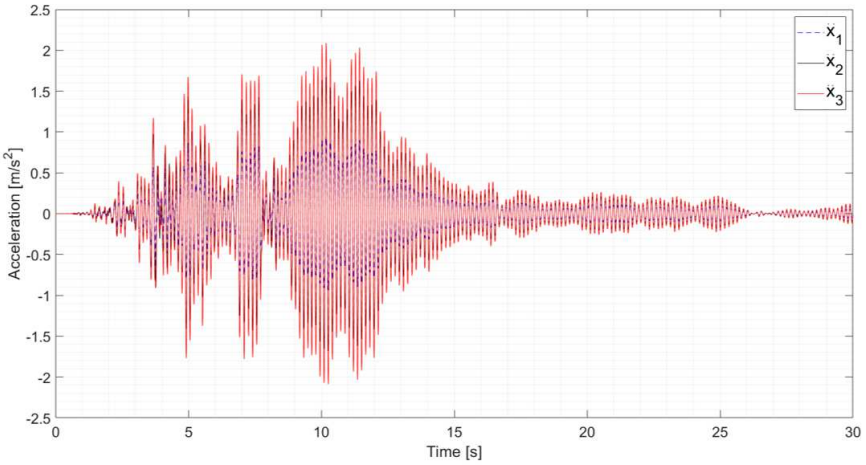


Fig. 18 Time-domain response of acceleration along the height of the 3-story structure under seismic excitation considering soil-structure interaction (SSI).

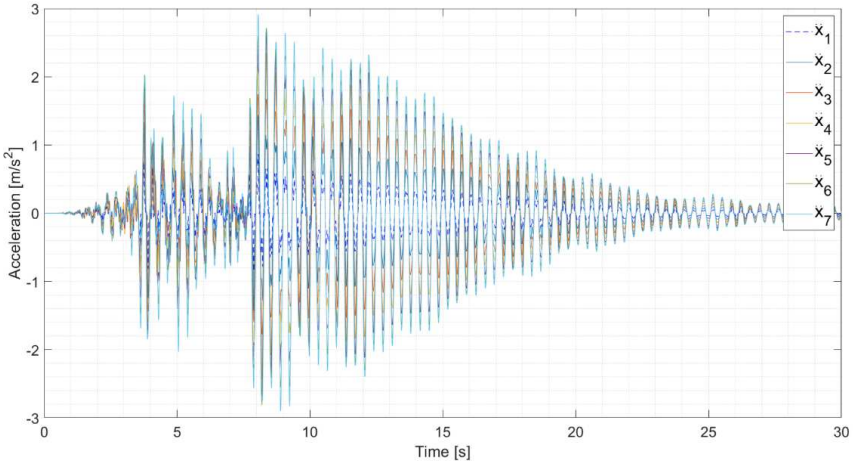


Fig. 19 Time-domain response of acceleration along the height of the 7-story structure under seismic excitation considering soil-structure interaction (SSI).

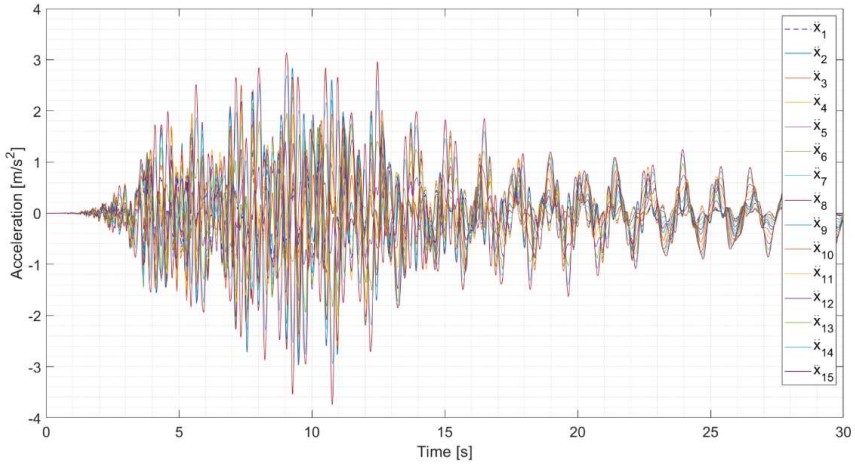


Fig. 20 Time-domain response of acceleration along the height of the 15-story structure under seismic excitation considering soil-structure interaction (SSI).

The Fast Fourier Transform (FFT) was applied to the responses obtained through the State-Space approach. The vibration amplitudes in the frequency domain, in terms of displacement and velocity for the three structures, are presented in Figures 21 to 26. Table 8 summarizes the maximum amplitude values for each analysed structure.

The results indicate that the largest vibration amplitudes in the frequency domain occur at the top floor of each structure and are predominantly associated with the fundamental vibration mode. As the number of floors increases, a clear shift of the dominant response toward lower frequencies is observed, which reflects the increase in global structural flexibility. This behavior highlights the strong influence of the fundamental mode on the dynamic response of taller structures.

Table 9 presents the computational processing time required by the State-Space method for the structural models with 3, 7, and 15 floors. Although the size of the matrices increases with the complexity of the models, the solutions are obtained within a relatively short computational time.

For comparison purposes, simulations using the Runge–Kutta method and the State-Space approach were performed for a seismic excitation case without soil–structure interaction (SSI), considering a two-dimensional structure with three floors. The processing time was approximately 415.36 s (about 7 minutes) for the Runge–Kutta method and 0.79 s for the State-Space formulation.

These results indicate that, for the uncoupled case, the State-Space approach is significantly more efficient. In the coupled case, although the computational time increases, it remains relatively low when compared to the processing time required by the Runge–Kutta method without considering soil effects.

Table 8 Responses of maximum vibration amplitudes in terms of displacement and velocity in the frequency-domain.

	3-story structure	**7-story structure**	**15-story structure**
D	0.0001171 m – 6.342 Hz	0.001519 m – 2.867 Hz	0.01947 m – 0.7953 Hz
V	0.004681 m/s – 6.362 Hz	0.02736 m/s – 2.867 Hz	0.09728 m/s – 0.7953 Hz

D: displacement; V: velocity.

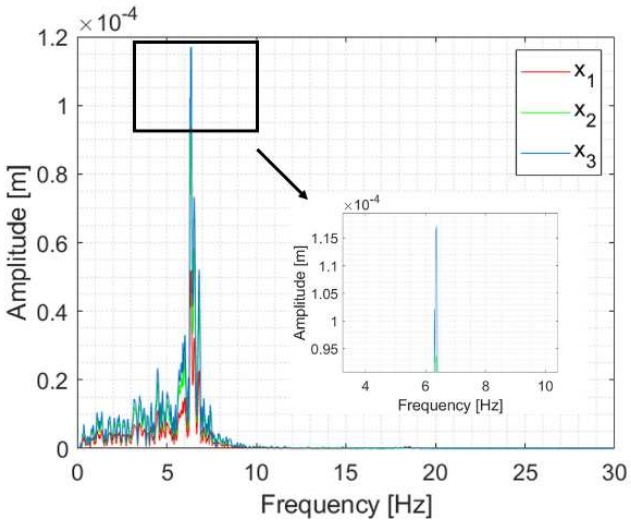


Fig. 21 Frequency-domain response of displacement for the 3-story structure under seismic excitation considering soil-structure interaction (SSI).

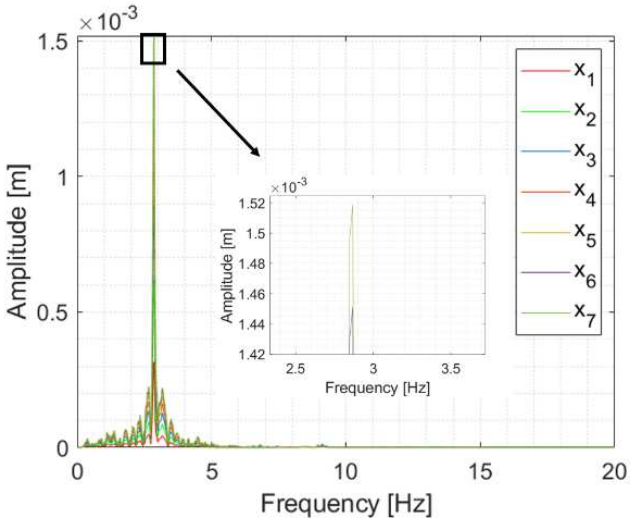


Fig. 22 Frequency-domain response of displacement for the 7-story structure under seismic excitation considering soil-structure interaction (SSI).

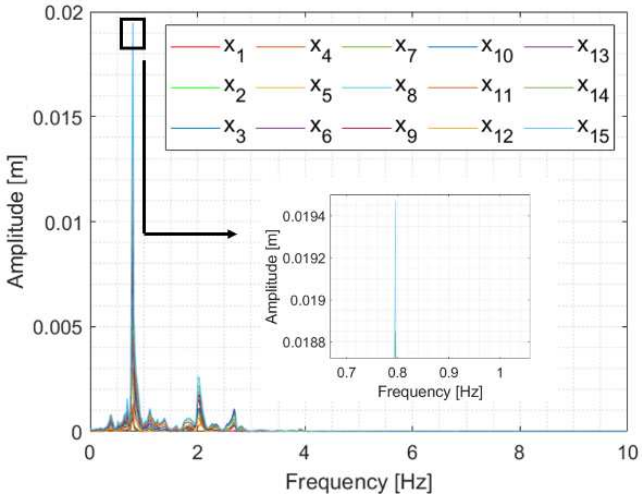


Fig. 23 Frequency-domain response of displacement for the 15-story structure under seismic excitation considering soil-structure interaction (SSI).

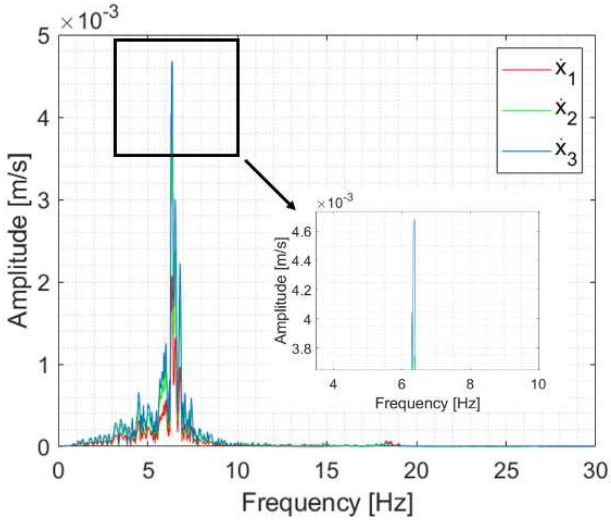


Fig. 24 Frequency-domain response of velocity for the 3-story structure under seismic excitation considering soil-structure interaction (SSI).

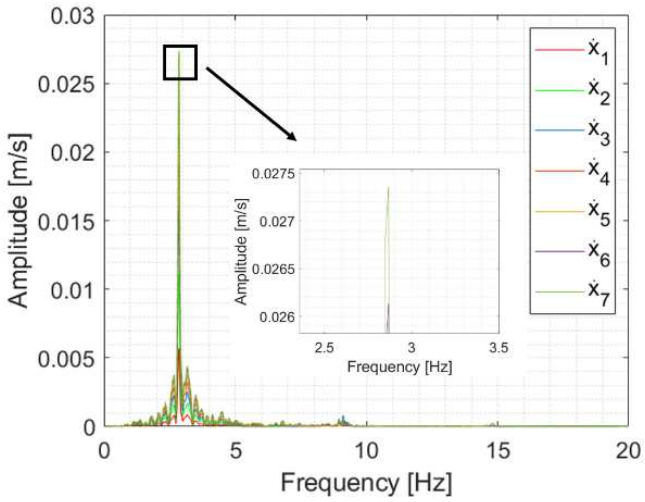


Fig. 25 Frequency-domain response of velocity for the 7-story structure under seismic excitation considering soil-structure interaction (SSI).

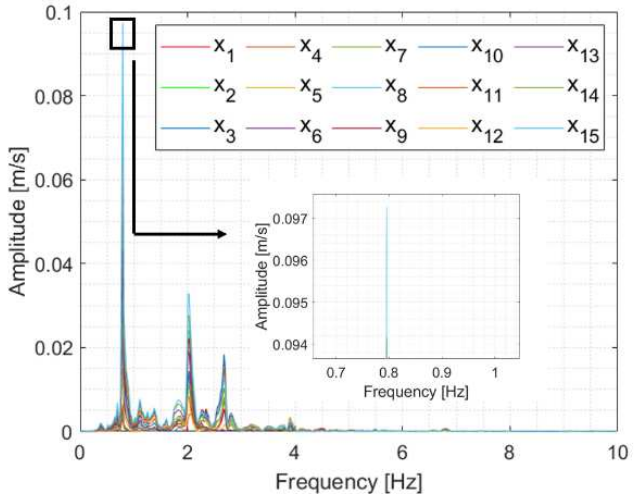


Fig. 26 Frequency-domain response of velocity for the 15-story structure under seismic excitation considering soil-structure interaction (SSI).

Table 9 Processing time of each structure.

	3-story structure	**7-story structure**	**15-story structure**
Time	9.623340 s	10.655012 s	38.326293 s

Most vibratory systems are inherently complex, and accurately predicting all the variables involved remains a challenging task. In this context, the State-Space formulation for two-dimensional problems, considering predominantly flexural structural behaviour, was presented through different applications as an efficient and versatile solution approach. The results demonstrated the feasibility of employing this method in problems involving soil–structure interaction (SSI) and seismic excitation.

The main difficulty associated with the method lies in the modeling stage, which requires a thorough understanding of the physical system under analysis. An accurate definition of the material properties and system matrices is essential, since any inconsistency in these inputs may lead to significant inaccuracies in the final results.

4 Conclusions

The State-Space approach proved to be a compelling alternative for solving dynamic problems, combining high computational efficiency with accuracy across the cases analysed. Its application to the three structural models provided a comprehensive evaluation of their dynamic behaviour in both time and frequency domains. The results confirmed that maximum displacements consistently occurred at the top floor, while the largest vibration amplitudes in the frequency domain were associated with the fundamental vibration mode.

The proposed formulation exhibited robustness for coupled soil–structure interaction problems under seismic excitation, demonstrating its potential as a reliable framework for dynamic structural analysis. Furthermore, the findings highlighted the significant influence of structural flexibility and soil properties on the overall dynamic response.

Future research should extend this formulation to three-dimensional analyses, incorporating nonlinear effects and a broader range of geotechnical parameters. Given that soil properties critically dictate the seismic response of coupled systems, more detailed investigations into soil–structure interaction (SSI) effects are highly recommended.

Supplementary information. No supplementary information is available for this article.

Acknowledgements. The first author gratefully acknowledges the financial support provided by the Coordenação de Aperfeiçoamento de Pessoal de Nível Superior (CAPES, Brazil), under Finance Code 001, through a master's scholarship.

The authors would like to thank the Universidade Tecnológica Federal do Paraná (UTFPR) for providing the infrastructure and support for conducting research on soil-structure interaction. Author Francisco would like to extend their gratitude

to the computational support of the FabLab-UTFPR/PB Consolidation project – Universidade Tecnológica Federal do Paraná (UTFPR-PB) - FINEP Reference - 1333/22.

Declarations. Funding: This study was financed in part by the Fundação Araucária de Apoio ao Desenvolvimento Científico e Tecnológico do Estado do Paraná, grant nº FEL2023301000051 - Reference CP 19/2023.

Conflict of interest/Competing interests: The authors declare no competing interests.

Ethics approval and consent to participate: Not applicable.

Consent for publication: Not applicable.

Data availability: The datasets used during the current study are available from the corresponding author upon reasonable request.

Materials availability: Not applicable.

Code availability: The MATLAB codes developed for this study are available from the corresponding author upon reasonable request.

Authors' contributions: Patricia Grezelle: Methodology, Software, Validation, Writing - Original Draft. Ana Raquel Pessa: Methodology, Writing - Original Draft, Writing - Review & Editing. Matheus Wessling: Methodology, Writing - Review & Editing. Francisco A. A. Gomes: Conceptualization of this study, Methodology, Formal analysis, Supervision. Paôla R. Dalcanal: Conceptualization of this study, Methodology, Formal analysis, Supervision. Paulo R. Novak: Conceptualization of this study, Methodology, Formal analysis, Supervision.

References

[1] Soriano, H.L.: Introdução à Dinâmica Das Estruturas. Elsevier, Rio de Janeiro (2014)

[2] Wolf, J.P.: Dynamic Soil-Structure Interaction. Prentice-Hall, Englewood Cliffs, New Jersey (1985)

[3] Kausel, E.: Early history of soil–structure interaction. Soil Dynamics and Earthquake Engineering **30**(9), 822–832 (2010) https://doi.org/10.1016/j.soildyn.2009.11.001

[4] Liratzakis, A., Tsompanakis, Y.: Impact of soil saturation level on the dynamic response of masonry buildings. Frontiers in Built Environment **4**(3), 1–14 (2018) https://doi.org/10.3389/fbuil.2018.00024

[5] Amini, F., Bitaraf, M., Eskandari Nasab, M.S., Javidan, M.M.: Impacts of soil-structure interaction on the structural control of nonlinear systems using adaptive control approach. Engineering Structures **157**, 1–13 (2018) https://doi.org/10.1016/j.engstruct.2017.11.071

[6] Jiang, W., Zhou, Y., Xie, W.C., Pandey, M.D.: Direct method for generating

floor response spectra considering soil-structure interaction. Journal of Earthquake Engineering **26**(10), 4956–4976 (2021) https://doi.org/10.1080/13632469.2020.1852137

[7] Wolf, J.P.: Dynamic Soil-Structure Interaction. Prentice-Hall, Englewood Cliffs, New Jersey (1988)

[8] Commandeur, J.J.F., Koopman, S.J., Ooms, M.: Statistical software for state space methods. Journal of Statistical Software **41**(1), 1–18 (2011) https://doi.org/10.18637/jss.v041.i01

[9] Ogata, K.: Modern Control Engineering. Prentice-Hall, New Jersey (2010)

[10] Kristensen, L.M.: State space methods for coloured petri nets. PhD thesis, University of Aarhus, Aarhus, Denmark (2000)

[11] Hutchinson, C.E.: The kalman filter applied to aerospace and electronic systems. IEEE Transactions on Aerospace and Electronic Systems **AES-20**(4), 500–504 (1984) https://doi.org/10.1109/TAES.1984.4502068

[12] Friedland, B.: Control System Design: An Introduction to State Space Methods. McGraw-Hill, New York (1986)

[13] Khakpour, M., Hajialilue Bonab, M.: Soil-structure-interaction using cone model in time domain for horizontal and vertical motions in layered half space. Journal of Earthquake Engineering **24**(4), 529–554 (2020) https://doi.org/10.1080/13632469.2018.1441766

[14] Wolf, J.P.: Foundation Vibration Analysis Using Simple Physical Models. Prentice-Hall, Englewood Cliffs, New Jersey (1994)

[15] MathWorks: MATLAB: The Language of Technical Computing, Version R2021a (2021)

[16] Eguchi, R.T., Goltz, J.D., Taylor, C.E., Chang, S.E., Flores, P.J., Johnson, L.A., Seligson, H.A., Blais, N.C.: Direct economic losses in the northridge earthquake: A three-year post-event perspective. Earthquake Spectra **14**(2), 245–264 (1998) https://doi.org/10.1193/1.1585998

[17] Nazarimofrad, E., Farahani, S., Zahrai, S.M.: Multiobjective optimal placement of active tendons to control irregular multistory buildings with soil-structure interaction. Structural Design of Tall and Special Buildings **28**(4), 1–18 (2019) https://doi.org/10.1002/tal.1581

[18] Grezelle, P., Gomes, F.A.A., Dalcanal, P.R., Carvalho, H.F., Novak, P.R., Bratti, G.: Numerical simulation of a three-dimensional structure considering the soil-structure interaction. In: Proceedings of the XLI Ibero-Latin-American Congress

on Computational Methods in Engineering (CILAMCE), Foz do Iguaçu, Brazil (2020)

[19] Pérez Peña, L.A.: Dynamic response of adjacent buildings: Considerations on soil-structure interaction. Master's thesis, University of Brasilia, Brasilia, Brazil (2017)

[20] Williams, R.L.I., Lawrence, D.A.: Linear State-Space Control Systems. John Wiley & Sons, New Jersey (2007)

[21] Chen, C.-T.: Linear System Theory and Design. Oxford University Press, New York (1998)

[22] Shultz, D.G., Melsa, J.L.: State Functions and Linear Control Systems. McGraw-Hill, New York (1967)

[23] Gilat, A., Subramaniam, V.: Numerical Methods for Engineers and Scientists: An Introduction to Applications Using MATLAB. Bookman, Porto Alegre (2008)

[24] Chapra, S.C., Canale, R.P.: Numerical Methods for Engineers, 6th edn. McGraw-Hill, New York (2010)

[25] Bowles, J.E.: Foundation Analysis and Design. McGraw-Hill, New York (1996)

[26] ABNT: NBR 6120: Actions for the Calculation of Building Structures, Rio de Janeiro (2019)

[27] Center, P.E.E.R.: PEER Ground Motion Database. https://ngawest2.berkeley.edu/site (2013)